

UNCLASSIFIED

Defense Technical Information Center
Compilation Part Notice

ADP013674

TITLE: Direct Numerical Simulation of Turbulent Mixing in a Rough-Wall Flow

DISTRIBUTION: Approved for public release, distribution unlimited

This paper is part of the following report:

TITLE: DNS/LES Progress and Challenges. Proceedings of the Third AFOSR International Conference on DNS/LES

To order the complete compilation report, use: ADA412801

The component part is provided here to allow users access to individually authored sections of proceedings, annals, symposia, etc. However, the component should be considered within the context of the overall compilation report and not as a stand-alone technical report.

The following component part numbers comprise the compilation report:

ADP013620 thru ADP013707

UNCLASSIFIED

DIRECT NUMERICAL SIMULATION OF TURBULENT MIXING IN A ROUGH-WALL FLOW

K. TSUJIMOTO, Y. MIYAKE AND N. NAGAI

*Department of Mechanical Engineering, Osaka University
2-1, Yamada-oka, Suita, 565-0871 JAPAN*

1. Introduction

Rough-wall turbulent flows are more common in engineering application than smooth-wall turbulent flows. Modification of mean flow and turbulence property have been established by enormous experiments. However, details of mechanism of rough-wall turbulence has been understood little because spatial resolution is limited in experiments. Meanwhile, Direct Numerical Simulation (DNS) of a rough-wall turbulent flows which is capable of giving high resolution data requires prohibitively heavy computer power and accordingly, no other DNS data are available than those published by the present authors (Miyake *et al.*, 1999). Our first DNS considered sand-grain roughness whose effect was implemented by profile drag based on Stokes drag and could successfully reproduce experimentally established rough-wall turbulent flow such as downward shift of straight line of logarithmic mean velocity distribution and vanishing of viscous sublayer. It was confirmed that the layer adjacent to the wall up to several tens in wall unit where smooth-wall turbulence exhibits autonomous property independent on the layer above it, is taken over by the layer having property of logarithmic layer, in rough-wall turbulence. While quasi-streamwise vortices play major role to generate high turbulent shear stress in this near-wall layer in smooth-wall turbulent flow, roughness destroy this vortical system and consequently, different mixing system which replaces the role of quasi-streamwise vortices should be found in rough-wall layer. Present work intends to investigate the turbulent mixing in the layer close to the wall of rough-wall turbulence by a DNS of more sound numerical conditions, *i.e.*, without using any model for roughness element.

Table 1. Computational conditions

	Streamwise	Wall normal	Spanwise
Length (wall unit)	$2\pi H$ (942)	$2H$ (300)	πH (471)
Grid number	256	257	128
Reynolds number	$Re_\tau = H\bar{u}_\tau/\nu = 150$		

2. Computational procedure

2.1. CHANNELS

Since implement of a roughness element in the calculation requires enormously high computational power, only one wall is assumed rough and the other, smooth. The configuration of the channel is illustrated in Fig.1. A Cartesian coordinate system is employed, in which x , y , z are streamwise, wall-normal, and spanwise directions, respectively, and the velocity components in the respective directions are denoted by u , v , w .

Computational conditions such as size of computational domain, grid number and Reynolds number are given in Table 1. The global Reynolds number is defined as $Re_\tau = \bar{u}_\tau H/\nu$ where \bar{u}_τ is global mean friction velocity and is calculated from pressure gradient $d\bar{p}/dx$ by $\bar{u}_\tau = [(H/\rho)(d\bar{p}/dx)]^{1/2}$, H is half channel width and ν and ρ are kinematic viscosity and density, respectively. In the following, superscript($\bar{\cdot}$) denotes quantities averaged in a plane parallel to the wall (x - z plane), superscript($'$), fluctuation from this mean and superscript($^+$), non-dimensionalized quantities by \bar{u}_τ which is mean friction velocity and ν . The spatial discretization is a Fourier series expansion in x and z for the sake of periodicity and a Chebyshev polynomial expansion in the normal direction. Time advancement is done by a semi-implicit method (Crank-Nicolson scheme for viscous term and third order Adams-Bashforth scheme for the convective term).

2.2. ROUGHNESS ELEMENT

The roughness is composed of periodically arranged two-dimensional spanwise ribs whose cross section is a square of a side $h_s^+ = 20$ and separated in streamwise direction by $\Delta x^+ = 118$. The boundary condition on the solid wall is treated rigorously to satisfy non-slip flow. Namely, at each grid point \mathbf{x}_s on every rib surface, external force \mathbf{f}_v is added so as to make the flow vanishing there. The magnitude of \mathbf{f}_v is determined iteratively to satisfy

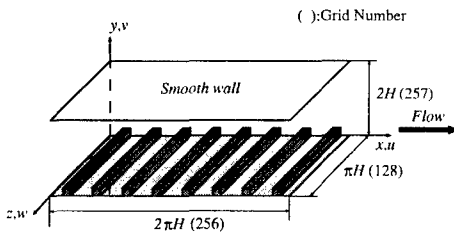


Figure 1. Configuration of a channel with a rough wall of 2-dimensional ribs.

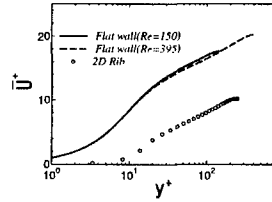


Figure 2. Distribution of mean velocity \bar{u}^+ normalized by mean friction velocity $\bar{u}_{\tau,r}$ on the rough wall and ν .

$$\mathbf{f}_v(\mathbf{x}_s, t) = \alpha_v \int_0^t \mathbf{v}(\mathbf{x}_s, t') dt' + \beta_v \mathbf{v}(\mathbf{x}_s, t) \quad (1)$$

where α_v and β_v are negative constants to prevent the computation from instability and in this calculation, they are $\alpha_v = -4 \times 10^5$ and $\beta_v = -6 \times 10^2$. These procedures are proposed by Goldstein *et al.* (1995).

3. Results

3.1. MEAN FLOW PROPERTY

Mean velocity distributions are given in Fig.2. In order to make the straight line of logarithmic part parallel to the one established for the ordinary smooth wall, correction of the location of wall surface is required. In this case, upward-shifting by $\Delta y^+ = 7.0$ is needed. Magnitude of the downward shift of the straight lines from the case of the ordinary smooth wall is within the scatter of experimental data (Raupach *et al.*, 1991). Corresponding shear stress distribution is given in Fig.3. The height H_r from the rough-wall where total shear stress vanishes is defined hereafter as the equivalent half width of the rough-wall channel. The width H_r is larger than H because total drag on the rough wall is larger than on the smooth wall. The defect of total shear stress in the layer close to the rough wall found in Fig.3 is covered by pressure drag of ribs. It is noted that local high viscous shear stress $\bar{\tau}_{wr}/\rho = \nu(\partial\bar{u}/\partial y)$ is observed in the layer near the top of the rib surface.

3.2. MODIFICATION OF LARGE-SCALE FLOW

The modification of large-scale flow by rough-wall is considered in this section, since it is substantial for global mixing. Figure 4 shows the ratio of turbulent shear stress $-\overline{u'v'}$ to turbulent kinetic energy k , $r = -\overline{u'v'}/k$.

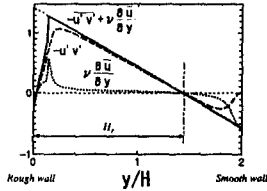


Figure 3. Distribution of shear stress across channel, normalized by overall mean friction velocity \bar{u}_τ and ν .

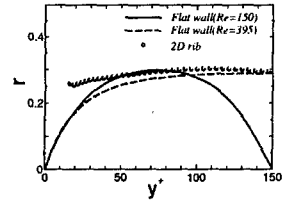
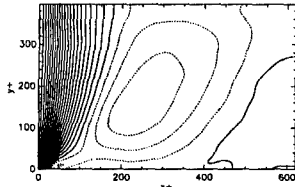
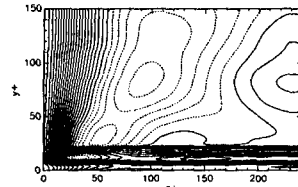


Figure 4. Distribution of structure parameter $r = -\overline{u'v'}/k$.



(a) smooth ($Re_\tau = 395$)



(b) 2D rough wall

Figure 5. Iso-contour of spanwise correlation factor of streamwise velocity fluctuation.

It is known to be around 0.27 in the logarithmic layer and the larger the Reynolds number, the thicker the constant r -layer. Present simulation shows that the wall roughness makes this layer to reach closer to the wall, as expected.

As mentioned earlier, the profile drag is dominant on the rough wall. However, in the region near the top of the roughness elements, the shear stress must be sustained mostly by turbulent shear flows. Therefore, strong turbulent mixing is required there. While quasi-streamwise vortices play dominant role for strong mixing near the smooth wall, rough-wall is expected to have different mechanism for the strong mixing. Figures 5 show the contour of spanwise correlation of streamwise velocity fluctuation. In place of streaks of mean spanwise separation $\Delta z^+ \sim 100$ which is a distinguished feature of the buffer layer, large scale streaks of much larger mean spanwise separation than in the buffer layer appears. These large-scale streaks are characteristic of wall turbulence of a large Reynolds number and accordingly, of the layer close to the wall near the rough surface. These observation suggests that the turbulence property normally found in the layer away from the wall prevails closer towards the wall in a rough-wall case. Namely it is suggested that a large-scale mixing takes place actively over the roughness.

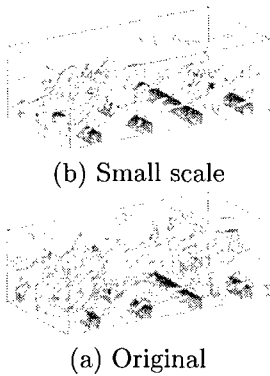


Figure 6. Iso- surface of the second invariance of velocity gradient tensor Q' ($Q'^+ > 1.8 \times 10^{-4}$).



Fig. 8 Extracted vortex structure LSE with the detector in the plane at $y^+ = 25$. (a) detector at near the rib, (b) position of detector unconditioned. ($Q'^+ > 1.8 \times 10^{-4}$).

3.3. TURBULENT MIXING DUE TO COHERENT VORTICES

To investigate the contribution of coherent vortices of different scale to turbulent shear stress, a filter is used to decompose the flow. The decomposing filter is of wavelengths of $\delta_x^+ \approx 400$, $\delta_z^+ \approx 100$ in x, z direction, respectively. Figure 6 compares (a) whole scale flow and (b) large-scale eddies discarded flow, by the iso-surfaces of the second invariance of velocity gradient tensor $Q'^+ = 1.8 \times 10^{-4}$. It is observed that the coherent flow mainly consists of small-scale eddies of above-defined length. Figure 7 which shows the contribution of each component to turbulent shear stress demonstrates that the shear stress is composed dominantly of the small scale vortices in near-wall region of both smooth- and rough-wall flow, especially in rough-wall flow and that the stress due to small-scale vortices is strongly enhanced over the rough-wall. An alternative way that we attempted to extract the governing event associated with the generation of turbulent shear stress is based on LSE (Linear Stochastic Estimation, Adrian *et al.*, 1988). The extracted

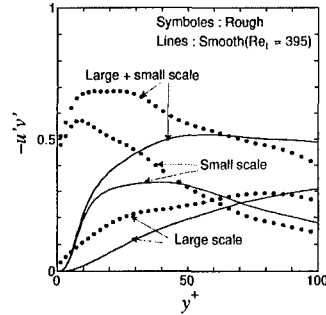
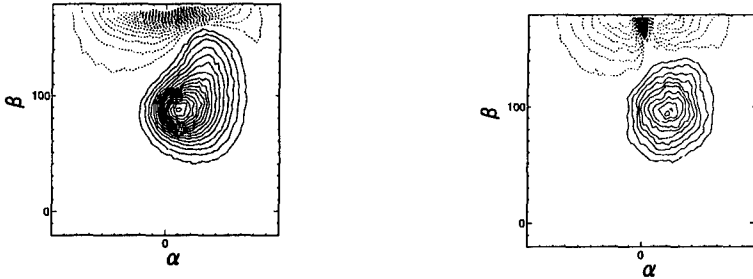


Figure 7. Distribution of separately averaged turbulent shear stress due to large and small-scale flow.



(a) Smooth wall at $Re_\tau = 395$ in $y^+ = 10 \sim 50$ (b) Rough wall in $y^+ = 10 \sim 50$

Figure 9. Contour lines of statistical property of vorticity on $\alpha - \beta$ plane. Solid lines : positive, dotted lines : negative.

structures in positioning the detector in the plane parallel to the wall at $y^+ = 25$ are shown in Fig.8 which demonstrate that streamwise elongated vortices are the key structures and that the key structure does not depend on the position of the detector, as in (b) which is for the detector's position unconditioned. It is also found that the extracted vortices are more tilted from the wall in the rough-wall case than in smooth wall case, though the pictures are not shown here. It is concluded that such a modulation of attitude angle of vortices is substantial in enhancing the turbulence mixing of near-wall layer, in rough-wall flow. In order to know the tilting property of the vortices, weighted average of a quantity $\hat{\phi}$ on the attitude angle of vortex line α, β is defined as,

$$\hat{\phi} = \int_V \int_{\beta-\Delta\beta}^{\beta+\Delta\beta} \int_{\alpha-\Delta\alpha}^{\alpha+\Delta\alpha} \phi(\alpha, \beta) d\alpha d\beta dV \quad (2)$$

where $\alpha = \tan^{-1}(\omega_y / \sqrt{\omega_x^2 + \omega_z^2})$, $\beta = \tan^{-1}(\omega_x / \omega_z)$, $\Delta\alpha = 2.5^\circ$, $\Delta\beta = 5^\circ$.

Figures 9 which shows the average for $\hat{\phi} = \hat{Q}$ gives the peak of Q in α - β map at around $\beta \approx 90^\circ$, which corresponds to streamwise small-scale vortices. In rough wall flow, the peak shifts to larger α than in smooth-wall flow, indicating that the vortex structures inclines more from the wall in average.

3.4. FORMATION OF SMALL-SCALE COHERENT VORTICES OVER THE ROUGHENED WALL

Though small-scale coherent vortices are found to be key structures of turbulence mixing over roughened wall, the well-known coherent vortices found in smooth wall flow are different however, from those of rough-wall flow.

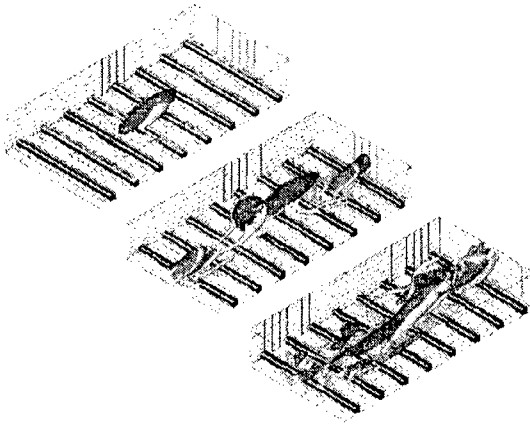


Figure 10. Evolution of a hairpin vortex initially introduced in a laminar flow having velocity distribution of a turbulent flow, $T^+ = 0, 120, 240$. Light color : $Q^+ > 0.0001$, Dark color : $u' < -2$

Visualization of the small-scale coherent vortices demonstrates diversity of vortices. In the region over the top of roughness element, it seems that vortex generation is strongly associated with the flow separation at the upstream corners of roughness elements, *via* a shedding of strong vortex sheets. However, complexity of flow structure does not allow us to trace the evolution of vortices. Therefore, to investigate the fundamental process of vortex formation, an evolution of a single hairpin vortex is traced by conducting numerical simulation in which a laminar flow having mean flow distribution of turbulent flow is assumed and small eddy is introduced in it at an initial time. The introducing baby eddy can be extracted by LSE as proposed by Zhou *et al.* (1996). Figures 10 show the evolution for the non-dimensional time $T^+ (= T\bar{u}_\tau^4/\nu^2) = 0, 120, 240$ and depict iso-surfaces of Q^+ and low-speed streaks. The vortex introduced initially is a pair of small quasi-streamwise vortices. At the beginning, the quasi-streamwise vortices grows quickly to a hairpin vortex and extends to further away from the wall. At $T^+ = 120$, the secondary hairpin vortex is born newly at the upstream of primary hairpin vortex, *i.e.*, regeneration is confirmed. At $T^+ = 240$, the group of vortices becomes matured and the size of the originally introduced vortex becomes larger than half width of the channel. Qualitatively, the evolution of vortices in the upper layer from the wall is similar to that of smooth wall case simulated in the previous work (Zhou *et al.* 1996, 1999 ; Miyake *et al.*, 2000). However, in the layer closest to the wall, a distinct pattern of vortex generation appears. In the smooth wall case, though not shown here, a lot of quasi-streamwise vortex are generated over the flat wall, most probably forming a vortex group. In rough wall case, instead of

such a group of quasi-streamwise vortices around the legs of primary hairpin vortex, vortex shedding at the upstream corner of roughness elements occurs induced by the vortical flow from upper layer. Although the ordinary regeneration process of smooth wall flow are destroyed in rough wall flow, strong vorticity from not random but fixed position associated with roughness supplements the loss and maintain turbulence. This characterizes the rough-wall turbulence as an alternative way of generating vortices, suggesting that regeneration of quasi-streamwise vortices by themselves is not always unique process.

4. Conclusions

1. The turbulence property normally found in the layer away from the wall prevails close to the wall and large-scale streaks comes closer to the wall. It is suggested that a large-scale mixing takes place over the roughness.
2. The major effect of roughness element is to modify the mechanism of turbulent mixing. Modulation of attitude angle of vortex which is tilted upward from the wall is the key factor in enhancing mixing in near-wall layer over the roughness.
3. On the observation of simplified simulation and the visualized instantaneous flow field of full simulation, further away from the wall, the mechanism of generation of coherent vortices is similar to that of smooth wall case. Closer to the top of roughness, however, quasi-streamwise vortices are not observed. The vortex sheet shedding at the upstream corner of roughness causes the vortex generation. Thus in rough-wall flow, regeneration process of the quasi-streamwise vortices by themselves is suppressed.

References

1. Adrian, R.J. and Moin, P., 1988, "Stochastic estimation of organized turbulent structure: Homogeneous shear flow", *J. Fluid Mech.*, **190**, pp.531-559.
2. Goldstein, D., Handler, R. and Sirovich, L., 1995, Direct numerical simulation of turbulent flow over a modeled riblet covered surface. *J. Fluid Mech.*, **302**, 598-606
3. Miyake, Y., Tsujimoto, K. and Agata, Y., 1999, A DNS of a turbulent flow in a rough-wall channel using roughness elements model. *JSME Intern.J.*, **43-2**, 233-242
4. Miyake, Y., Tsujimoto, K., Sato, N. and Suzuki, Y., 2000, Turbulence Property in the Near-Wall Layer. *Trans JSME, ser B* **66-650**, 2585-2592 (in Japanese)
5. Raupach, M.R., Antonia, R.A. and Rajagopalan, S., 1991, Rough-wall boundary layers. *Appl. Mech. Rev.*, **44-1**, 1-25
6. Zhou, J., Adrian, R.J. and Balachandar, S., 1996, "Autogeneration of near-wall vortical structures in channel flow", *Phys. Fluids*, **8-1**, pp.288-290.
7. Zhou, J., Adrian, R.J., Balachandar, S. and Kendall, T.M., 1999, "Mechanism for generating coherent packets of hairpin vortices in channel flow", *J. Fluid Mech.*, **387**, pp.353-396.